The Effect of a Revised Beaufort Equivalent Scale on Momentum and Heat Fluxes over the Global Oceans

Christine C. Young
National Oceanographic Data Center, NOAA

Arlindo M. da Silva
Data Assimilation Office, NASA/GSFC

and

Sydney Levitus
National Oceanographic Data Center, NOAA

Abstract

Using individual observations from the COADS Compressed Marine Reports (Slutz et al. 1985), we have computed revised global climatologies and anomalies of wind stress and heat fluxes. The flux computations utilize a revised Beaufort equivalent scale for estimated wind speeds, use wind speed reduced from an average anemometer height to 10 m above sea level, and include Large and Pond (1981, 1982) transfer coefficients.

The magnitude of the revised climatological mean wind stress is smaller than estimates by previous authors, particularly in the Northern Hemisphere extratropics. The revised heat fluxes appear to overestimate insolation and underestimate evaporation. Using linear inverse theory, we have constrained the heat fluxes to balance globally. These constrained heat fluxes produce heat transport in the Atlantic in agreement with oceanographic measurements.

Introduction

In a companion paper, da Silva et al. (1995, this volume) discussed the development of a new Beaufort equivalent scale. This scale was developed in an attempt to bring measured and estimated wind speeds in COADS (Slutz et al. 1985) into closer agreement. When this revised scale is applied to individual observations, the climatological wind speed increases compared to uncorrected winds, but the wind speed standard deviation decreases. When the revised scale is used for wind stress calculation, climatological wind stress decreases over large areas of the oceans. This effect is primarily due to the decrease in wind standard deviation. When the revised scale is used for latent and sensible heat fluxes, latent heat flux is slightly larger than

the unrevised latent heat flux, and the revised sensible heat flux slightly smaller. In this paper we review the wind stress and heat flux products we have calculated using COADS individual observations and our revised Beaufort equivalent scale. We also describe the standard COADS Monthly Trimmed Summaries versus our revised COADS Monthly Summaries, and we show the impact of the revised scale on wind stress and compare this resulting wind stress to that of other authors. We evaluate the impact of the new scale on heat fluxes, explain the derivation of the constrained heat flux product and compare this constrained product to the heat fluxes of other authors. The last part contains a summary of the important points of the study.

Products

The standard COADS Monthly Trimmed Summaries (MTS) are as follows (Slutz et al., 1985): Means and statistics are calculated globally in $2° \times 2°$ latitude-longitude squares. No objective analysis is available with the standard release of COADS; the statistics are unfiltered and unsmoothed (although Oort and Pan [1986] applied an objective analysis to some of the $2° \times 2°$ statistics). The observed quantities are winds, sea level pressure, surface sea and air temperature, specific humidity, cloudiness, among others. Derived quantities include zonal and meridional momentum and heat fluxes as well as other quantities. For any of the quantities involving wind, the WMO Code 1100 Beaufort equivalent scale is used to convert the Beaufort force wind estimates to wind speed. The derived quantities which can be used for oceanic forcing are pseudo wind stress: W_u, W_v, and pseudo heat fluxes: $W(T_c - T_a)$, $W(q_s - q)$. To properly use these fields as forcing quantities one can assume the transfer coefficients are constant or introduce wind speed/stability effects using monthly means with the so-called classical method.

The revised COADS Monthly Summaries we have produced differ from the standard MTS in several ways: only means, standard deviations, and number of observations are available on a $1° \times 1°$ grid over the global ocean. In addition, an objective analysis has been applied to the means and standard deviations in order to fill in empty ocean squares and filter out noise. The analysis we use is a successive correction scheme with a Barnes response function-the same as used in Levitus (1982). We have the same observed quantities as the MTS and many of the same derived quantities. Our set also contains a few quantities, such as precipitation and shortwave radiation, that the MTS lack. For any quantities involving wind speed, we use our revised Beaufort equivalent scale. While the MTS provide pseudo heat and momentum fluxes, our product provides shortwave and longwave radiation to/from the sea surface in addition to latent/sensible heat flux and wind stress. These two radiation terms are not included in the MTS. Table 1 is a list of all fields we have calculated from the COADS individual observations.

For use as oceanic forcing terms, we have computed climatologies and anomalies of wind stress and heat fluxes using wind speed dependent and stability dependent transfer coefficients. We use the Large and Pond (1981, 1982) formulations for C_D, C_T, C_E. If a wind observation is estimated, we correct it using our revised scale. We then reduce the estimated or measured wind speed observation to 10 m before computing the transfer coefficients.

Wind Stress

The bulk formulation for wind stress is as follows:

$$\tau = \rho C_D W_{10} u_{10}$$

$$u_{10} = (u_{10} v_{10}), (at \ \ 10m)$$

$$W_{10} = \sqrt{u_{10}^2 + v_{10}^2}$$

$$C_D = C_N(W_{10}) f(Z/L), (drag \ \ coefficient)$$

$$C_N = neutral \ \ drag \ \ coefficient$$

$$f = stability \ \ correction$$

$$Z = 10m$$

$$L = Monin - Obukhov \ \ length$$

$$L = L(W, T_a, T_s - T_a, q_s - q)$$

Note that the drag coefficient is composed of the neutral drag coefficient and a stability correction. The neutral drag coefficient is a function of wind speed at 10 m. The stability correction is a function of the height (10 m) and the Monin-Obukov length. We convert the wind speed from the average anemometer height of 20 m to 10 m using standard surface layer similarity theory. If a wind observation was measured from a buoy, we convert the wind speed from 5 m to 10 m.

Effect of Corrections

To compare the effect of the revised Beaufort scale on wind stress, we compute two wind stress products. The first, revised or corrected wind stress, is calculated as explained above. The second, uncorrected, is computed the same as above except that the WMO Code 1100 scale is used for estimated winds and the anemometer height is assumed to be 10 m (i.e. no correction is made for height).

Figure 1 shows the global zonal means of the winter (DJF) zonal wind stress. Although the fields we calculate are global, we show only 60°S through 60°N here. This figure shows the revised wind stress as defined previously and the unrevised wind stress (in W/m^2). Notice that in large areas of the extratropics, the corrected (revised) wind stress is less than the

uncorrected wind stress. Although wind speed increases when the revised scale is applied, the wind stress decreases in many areas. This is mainly due to the large decrease in the standard deviation of the wind speed.

Comparison with Other Authors

We compare our revised wind stress to the fields computed by other authors by studying the response of a simple model. The linear, barotropic model of Fanning et al. (1994) of the North Atlantic ocean using smoothed topography was forced with our revised wind stress fields. We compare the seasonal transport anomaly through the Florida Straits in response to four different wind stress estimates (part of this comparison can be found in Fanning et al. 1994). Figure 2 shows the transport anomaly at the Florida Straits as calculated from cable measurements (Larsen 1992) and as calculated in response to four different wind stress estimates:

1. Hellerman and Rosenstein (1983) who use ship winds and a rather large estimate for C_D.

2. Trenberth et al. (1990) who use ECMWF 1000 mb winds as surface winds and the Large and Pond (1981) formulation for C_D.

3. Isemer and Hasse (1987) who correct Bunker's (1976) monthly mean values of wind stress (large C_D)

4. Our corrected wind stress as explained in this paper.

The transport from the Isemer and Hasse wind stress has the largest anomaly. This is expected due to the large CD in the Bunker data and their Beaufort scale correction which increases wind stress. Our wind stress estimate produces the smallest transport anomaly of all. This results from the relatively small Large and Pond C_D and our Beaufort/anemometer height correction which decreases wind stress over large parts of the North Atlantic. For this particular model, our corrected wind stress appears to underestimate ocean transport in the North Atlantic.

We have also compared our wind stresses, over time, to pseudo wind stresses derived by Servain and Lukas (1990) and Goldenberg and O'Brien (198 1). Figure 3 shows the temporal correlation between the pseudo stress magnitudes in northern winter (DJF) over two regions: the Tropical Atlantic and the Tropical Pacific. Figure 3 is the correlation between our wind stress and the Servain and Lukas (1990) pseudo wind stress over the Tropical Atlantic. Note that several large areas have correlations exceeding 80% and correlations in most areas exceed 60%. Areas which. have lower correlations tend to be regions in which there are few observations. Temporal correlations in the Tropical Pacific (Figure 4) between our wind stress and the pseudo stress of Goldenberg and O'Brien (1981) are not as high. This is not unexpected due to the scarcity of observations in the equatorial Pacific. Farther away from the Equator,

where the observation density is higher, the correlations are higher. This is particularly evident in the northern hemisphere.

Heat Fluxes

Using the COADS individual observations, we have also computed the four components of net heat flux: latent heat flux, sensible heat flux, incoming shortwave radiation, and outgoing longwave radiation. When computing latent and sensible heat flux, we use our revised Beaufort equivalent scale, reduce the winds to 10 m, and use Large and Pond's (1982) transfer coefficients.

Revised Scale and Constrained Product

An accurate estimate for net heat flux will produce a physically consistent global heat balance. Here we check the consistency of our revised net heat flux. The vertically integrated heat budget equation for the oceans is

$$\frac{\partial H}{\partial t} + \nabla \bullet H \; = \; Q_{net}$$

where

H = Heat content

H = Heat transport

Q_{net} = Net heat flux at the surface

$= Q_{SW} - (Q_{LW} + Q_L + Q_S)$

Integrating over many years we assume the heat storage vanishes:

$$\nabla \bullet \overline{H} \; = \; \overline{Q}_{net}$$

Neglecting the heat storage, the average annual net heat flux over the global oceans must be zero:

$$\iint_{Globe} \overline{Q_{net}} dx dy \; = \; 0$$

But, because $\overline{Q_{net}}$ is computed as difference of large, uncertain terms, the condition above is not met. Figure 5 shows the mean annual net heat flux over the global ocean (in W/m^2). It is clear that the amount of outgoing (negative) heat flux is not sufficient to balance the amount of incoming (positive) heat flux.

However, “small” adjustments in the bulk formulas can produce a physically consistent net heat flux. Following the method of Isemer et al. (1989), we use linear inverse theory (Menke 1984) to introduce non-dimensional correction factors to the bulk formulas. We assign a correction factor p to each term which is likely to be a source of error:

$$Q_{SW} = p_{Tr} Q_{clear} (1 - p_c 0.62c + 0.0019\beta)(1 - \alpha)$$

$$Q_{LW} = \varepsilon\sigma T_s^4 p_e (0.39 - 0.05\sqrt{e})\left(1 - p_X X c^2\right) + 4\varepsilon\sigma T_s^3 (T_s - T\alpha)$$

$$Q_L = p_L \rho c_p L_E C_E W (q_s - q)$$

$$Q_S = p_S \rho c_p C_T W (\theta_s - \theta)$$

We choose the transmissivity term of the clear sky radiation and the cloudiness term as likely sources of error in the shortwave formula (Q_{SW}). For longwave radiation (Q_{LW}), we choose the vapor pressure term and the cloudiness coefficient. For latent and sensible heat (Q_L,Q_S) we combine the errors likely to be found in the transfer coefficients and the difference terms and assign a single correction factor to each of the two fluxes. We assume that each error is statistically independent of the others. In the original calculation of heat flux, the factors P_{Tr}, P_c, P_e, P_X, P_L, and P_S are each equal to one. The goal is to find small corrections to the p’s so that the meridional heat transport, H, is consistent with oceanographic measurements. We use linear inverse theory to calculate the small corrections. In order for the solution to be acceptable, the corrections to the p’s must be smaller than the error allowance for each correction factor. We set the error limit for the latent and sensible heat flux factors to be 20%. The rest of the factors are allowed 10% error which is the approximate error for meridional heat flux measurements. As an example, we calculate the corrections so that the global meridional heat flux is constrained to zero at the southern boundary:

$$\delta p_{Tr} = -7\%$$

$$\delta p_c = +4\%$$

$$\partial p_e = +2\%$$

$$\delta p_X = -1\%$$

$$\delta p_L = +15\%$$

$$\delta p_s = +1\%$$

These corrections are smaller than the allowed error and thus are acceptable. The corrections serve to reduce shortwave radiation and increase evaporation. This finding is consistent with what Oberhuber (1988) did in order to balance his calculation of net heat flux, which was based on the classical method.

Figure 7 shows the constrained meridional heat transport using the corrections listed above. The transport (in 10^{15} W) is shown for the global ocean and for each individual ocean. Three measurements of meridional transport in the Atlantic are also shown. Our constrained Atlantic transport is within the error bars of Wunsch's (1984) and Hall and Bryden's (1982) measurements. Our Atlantic transport does not approach the measurement of Rago and Rossby (1987) who admit their measurement to be rather large. Figure 6 shows the constrained annual mean net heat flux. The negative and positive regions of net heat flux (in W/m^2) now balance out globally; the equilibrium considerations are met.

Comparison with Other Authors

The main component of the outgoing portion of net heat flux is the latent heat flux. For simplicity we compare our constrained latent heat flux to other authors. Figure 8 shows zonal averages of global latent heat flux (in W/m2) in winter for various authors. Our revised latent heat flux, labeled "UWM" is shown in comparison to Oberhuber (1988), and Esbensen and Kushnir (1981), whose data are obtained from ship observations. We also compare our flux to the latent heat flux estimated by Busalacchi et al. (1993) derived from SSM/I satellite measurements of winds with fields of temperature and moisture from the Goddard Laboratory for Atmospheres Fourth-Order General Circulation Model.

In general, our revised, constrained latent heat flux is greater than that derived by other authors. This is mainly due to the 15% increase in latent heat flux obtained when we apply the constraint parameters. The latent heat flux of the other authors only exceeds our constrained flux in two regions. The first is south of about 40°S where the derived fields are unreliable due to low observation density (with the probable exception of SSM/I). The second region in which our latent heat flux is less than the other authors' is in the northern hemisphere extratropics. Our revised latent heat flux tends to be less than Oberhuber's (1988) estimate north of around 35°N. Oberhuber used a value for Chamock's constant nearly six times the value we use. This increases his latent heat flux estimate significantly in regions where the friction velocity is high, namely north of around 30°N in the Atlantic and Pacific during the northern hemisphere winter.

Our revised latent heat flux is generally greater than that of Esbensen and Kushnir (198 1), who calculated their flux using the classical method. In some cases, this method can produce latent heat flux values greater than the method using individual observations (Esbensen and Reynolds 1981). At low to moderate wind speeds, their transfer coefficients (Liu et al. 1979) tend to be much smaller than our transfer coefficients in unstable conditions, but slightly larger in neutral or stable conditions. As the winter marine atmosphere is definitely unstable north of 40°N. it appears that the Esbensen and Kushnir latent heat flux is greater than or equal to ours north of 45°N due to either their monthly mean calculations or a difference in the data sets.

The SSM/I latent heat flux is greater than our revised latent heat flux north of 20°N. A similar pattern does not exist in the sensible heat flux which tells us that the excess is not due to a wind speed difference. The difference must lie in the analyses of temperature and/or moisture. Compared to Isemer and Hasse (1987) [comparison not shown] our latent heat flux is smaller. This is due to the same reasons that their wind speed exceeded our revised wind

speed: the Large and Pond transfer coefficients that we use tend to be smaller than their coefficients and their Beaufort correction tends to increase wind speeds by a larger amount than does our correction.

Concluding Remarks

Our revised wind stress fields, computed from COADS individual observations using our revised Beaufort equivalent scale, Large and Pond transfer coefficients, and the anemometer height reduction, are smaller than previous estimates. The revised stresses "under estimate" the transport anomaly through the Florida Straits in a linear barotropic model. However, a study in progress shows that, used in a tropical model, the revised stresses produce a realistic climatology and interannual variability of sea surface temperature in the Tropical Atlantic ocean.

Heat fluxes computed solely from the bulk formulas appear to overestimate shortwave radiation and underestimate evaporation. Thus they are not able to satisfy global equilibrium conditions. By using simple linear inverse theory we can impose small corrections upon the bulk formulas to produce heat transports in agreement with some oceanographic measurements. Our constrained latent heat flux is generally greater than the latent heat fluxes of other authors.

Acknowledgments

We would like to thank A. Fanning for kindly running his model with our revised stress. Work presented in this paper has been supported by NSF grant ATM 9215811 (AMdS/CCY) and by NOAA's Climate and Global Change Program (SL/CCY).

References

Busalacchi, A. J., R. M. Atlas, E. C. Hackert, 1993: Comparison of special sensor microwave imager vector wind stress with model-derived and subjective products for the tropical Pacific. *J. Geophys. Res*., 98, 6961-6977.

Bunker, A. F., 1976: Computations of surface energy flux and annual air-sea interaction cycles of the North Atlantic Ocean. *Mon. Wea. Rev*., 104, 1122-1140.

Esbensen, S. K., and Y. Kushnir, 1981: The heat budget of the global oceans: An atlas based on estimates from marine surface observations. Oregon State University Climate Research Institute Rep. No. 29, 27 pp.

Esbensen, S. K., and R. W. Reynolds, 1981: Estimating monthly averaged air-sea transfers of heat and momentum using the bulk aerodynamic method. *J. Phys. Oceanogr*., 11, 457-465.

Fanning, A. F., R. J. Greatbach, A. M. da Silva and S. Levitus, 1994: Model-calculated seasonal transport variations through the Florida Straits: A comparison using different wind-stress climatologies. *J. Phys. Oceanogr*., 24, 30-45.

Goldenberg, S. B., and J. J. O'Brien, 198 1: Time and space variability of tropical Pacific wind stress. *Mon. Wea. Rev*., 109,.1190-1207.

Hall, M. M., and H. L. Bryden, 1982: Direct estimates and mechanisms of ocean heat transport. *Deep-Sea Res*., 29, 339-359.

Hellerman, S., and M. Rosenstein, 1983: Normal monthly wind stress over the World Ocean with error estimates. *J. Phys. Oceanogr*., 13, 1093-1104.

Isemer, H.J., and L. Hasse, 1987: The Bunker Atlas of the North Atlantic Ocean. Vol. 2: Air-sea Interactions. Springer Verlag, 252 pp.

Isemer., H.-J., J. Willebrand and L. Hasse, 1989: Fine adjustment of large air-sea energy flux parameterizations by direct estimates of ocean heat transport. J Climate, 2, 1173-1184.

Large, W., and S. Pond, 19 8 1: Open ocean momentum flux measurements in moderate to strong winds. *J. Phys. Oceanogr*., 11, 324-336.

Large, W., and S. Pond, 1982: Sensible and latent heat flux measurements over the ocean. *J. Phys. Oceanogr*., 12,464-482.

Larsen, J. C., 1992: Transport and heat flux of the Florida Current at 27'N derived from cross-stream voltages and profiling data: Theory and observations. *Phil. Trans. Roy. Soc*. London A, 338, 169-236.

Levitus, S., 1982: Climatological Atlas of the World Ocean, NOAA Prof. Paper No. 13, US Government Printing Office, Washington DC, 17 fiches, 173 pp.

Liu, W. T., K. B. Katsaros and J. A. Businger; 1979: Bulk parameterization of air-sea exchanges of heat and water vapor including the molecular constraints at the interface. *J. Atmos. Sci*., 36, 1722-1735

Menke, W., 1984: *Geophysical Data Analysis: Discrete Inverse Theory*. Academic Press, 257 pp.

Oberhuber, J. M., 1988: An Atlas Based on the COADS Data Set: The Budgets of Heat, Buoyancy, and Turbulent Kinetic Energy at the Surface of the Global Ocean. Report No. 15, Max-Planck Institut fur Meteorology.

Oort, A. H., and Y.-H. Pan, 1986: Diagnosis of historical ENSO events. Programme on Long-Range Forecasting Research, No. 6, Vol. 1, WMO/TD-No. 87, World Meteorological Organization, 249-258.

Rago, T. T., and H. T. Rossby, 1987: Heat transport into the North Atlantic Ocean north of 27°N latitude. *J. Phys. Oceanogr*., 17, 854-871.

Servain, J., and S. Lukas, 1990: Climatic Atlas of the Tropical Atlantic Wind Stress and Sea Surface Temperature 19851989. IFREMER, SDP, Brest, France, 143 pp.

Slutz, R. J., S. J. Lubker, J. D. Hiscox, S. D. Woodruff, R. L. Jenne, D. H. Joseph, P. M. Steurer and J. D. Elms, 1985: COADS, Comprehensive Ocean-Atmosphere Data Set, Release 1. Climate Research Program, Environmental Research Laboratory, Boulder, CO 262 pp.

Trenberth, K. E., W. G. Large and J. G. Olson, 1990: The mean annual cycle in global ocean wind stress. *J. Phys. Oceanogr*., 20, 1742-1760.

Wunsch, C., 1984: An eclectic Atlantic Ocean circulation model. Part 1: The meridional flux of heat. *J. Phys. Oceanogr*., 14, 1712-1733.4

Table 1: **Variables in the UWM/COADS data set.**

File Name	Units	Description
airdens.nc	kg/m^3	sea level air density
bouy5.nc	$kg/(m^{3)}$	constrained bouy flux
cloud.nc	fraction of 1.	fractional cloudiness
evaprate.nc	mm/(3 hours)	evaporation rate
fvcubed.nc	m^{3}/s^3	ocean friction velocity cubed
icemask.nc	(none)	icemask
latent3.nc	W/m^2	corrected latent heat flux
longrad.nc	W/m^2	outgoing longwave radiation
netheat5.nc	W/m^2	constrained net heat flux
precip6.nc	mm/(3 hours)	precipitation rate
qair.nc	g/kg	specific humidity
qs_qa.nc	g/kg	qsea minus qair
qsea.nc	g/kg	sea level specific humidity
rh.nc	%	relative humidity
sat.nc	C	sea level air temperature
sensib3.nc	W/m^2	corrected sensible heat flux
shortrad.nc	W/m^2	incoming short wave radiation
slp.nc	mb	sea level air pressure
sst_sat.nc	C	sea minus air temperate
sst.nc	C	surface temperature
taux3.nc	N/m^2	corrected zonal wind stress
tauy3.nc	N/m^2	corrected meridional stress
u3.nc	m/s	corrected zonal wind
ua.nc	K m/s	zonal heat flux
uq.nc	m/s	zonal moisture flux
v3.nc	m/s	corrected meridional flux
va.nc	K m/s	meridional heat flux
vappress.nc	mb	vapor pressure
virtemp.nc	C	virtual temperature
vq.nc	m/s	meridional moisture flux
w3.nc	m/s	corrected wind speed
zdl.nc	(unitless)	10m/(Monin Obukov length)

Figure 1: Zonal wind stress averaged zonally over the glove (N/m2) for boreal winter (DJF). Revised stress (Corrected, solid line) is computed using the revised Beaufort scale with anemometer height reduction to 10 m. Uncorrected (broken line) stress is computed using the WMO Code 1100 without anemometer height reduction.

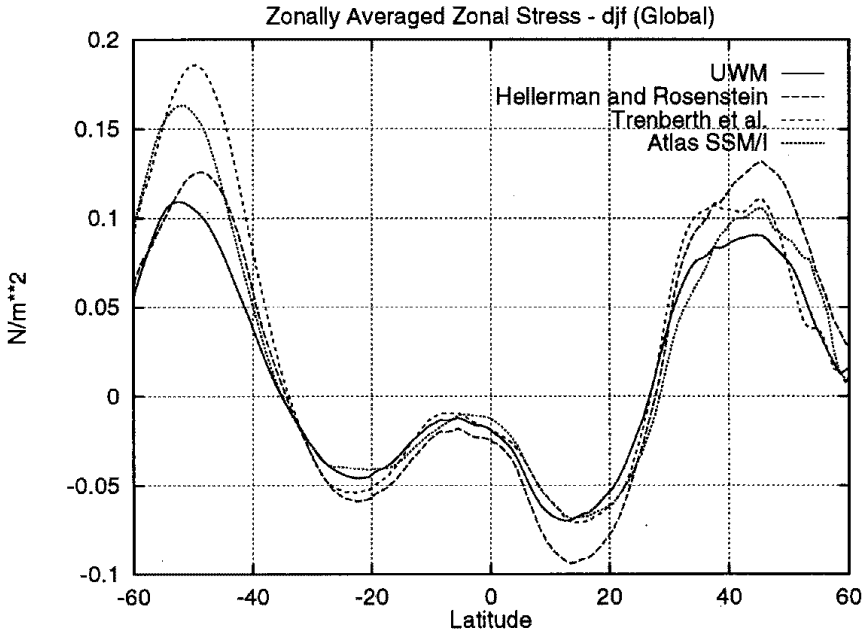

Figure 2: Transport anomaly (Sv) through the florida Straits observed from cable measurements (shown with error bars) [Larsen 1992] and from a linear barotropic model using smoothed topography. Modeled transport is in response to wind stress fields from (IH) Isemer and Hasse [1987], (HR) Hellerman and Rosenstein [1983]. (TR) Trenberth et al., [1990], and our (DS) corrected wind stress.

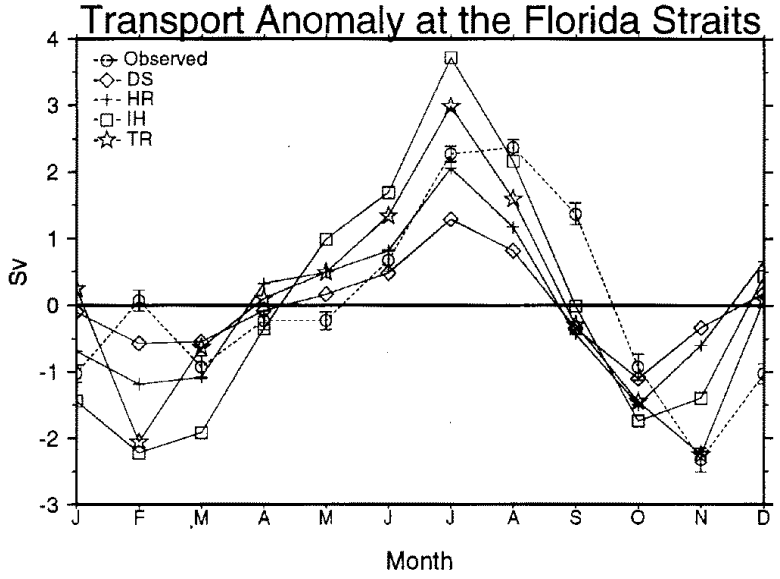

Figure 3: Correlation (%) between our revised wind stress and pseudo wind stress derived by Servain and Lukas (1990) for winter (DJF).

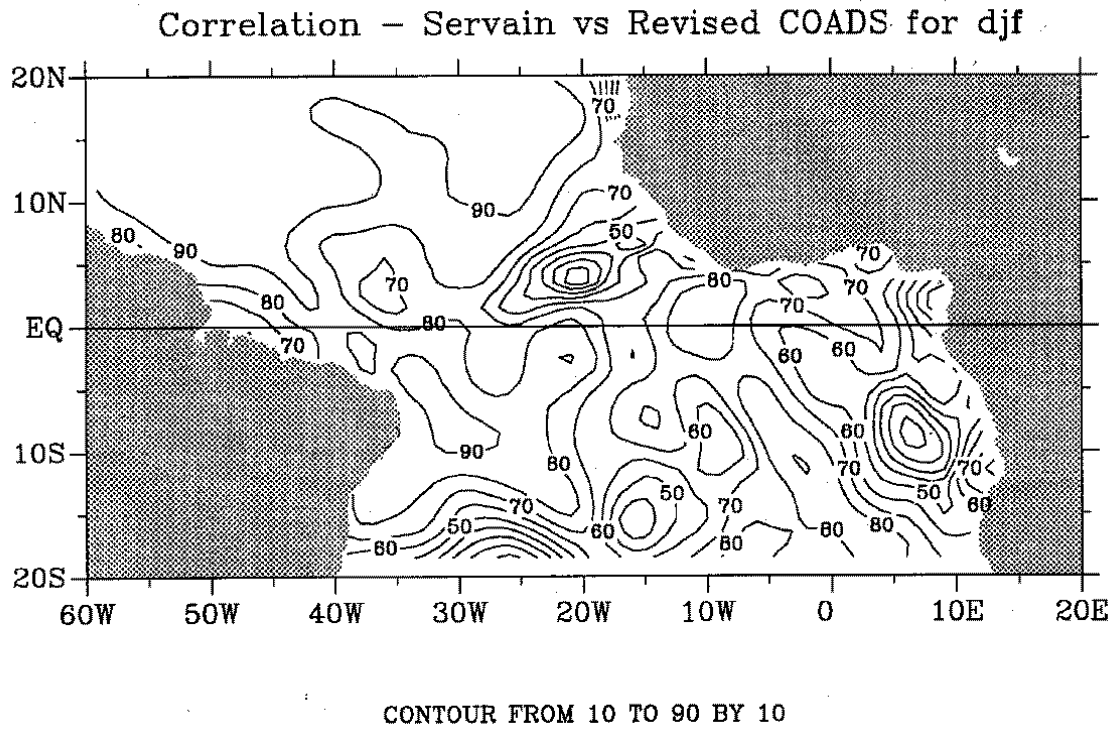

Figure 4: Correlation (%) between our revised wind stress and pseudo wind stress derived by Goldenberg and O'Brien (1981) for winter boreal (DJF).

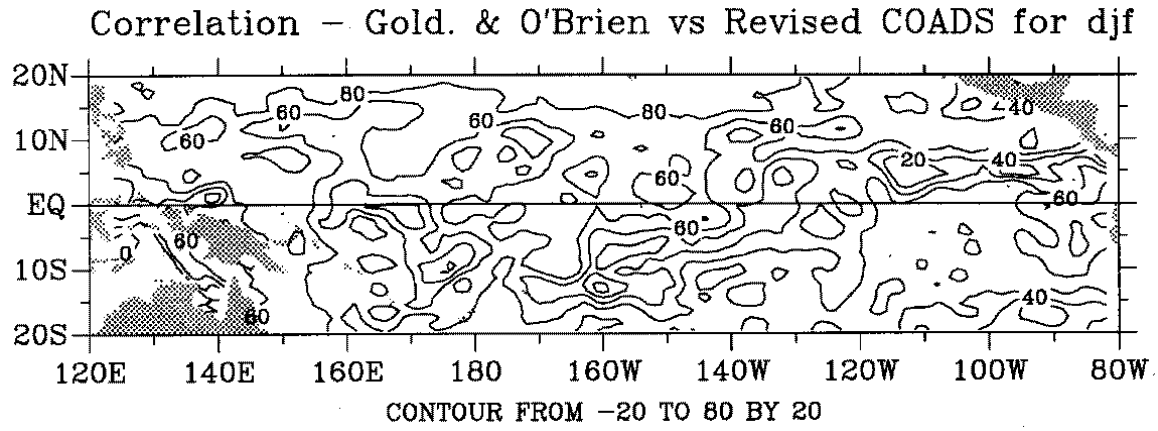

Figure 5: Revised, but unconstrained annual mean net heat flux over the global ocean (W/m^2). Heat flux is computed using the revised Beaufort scale with anemometer height reduction to 10 m.

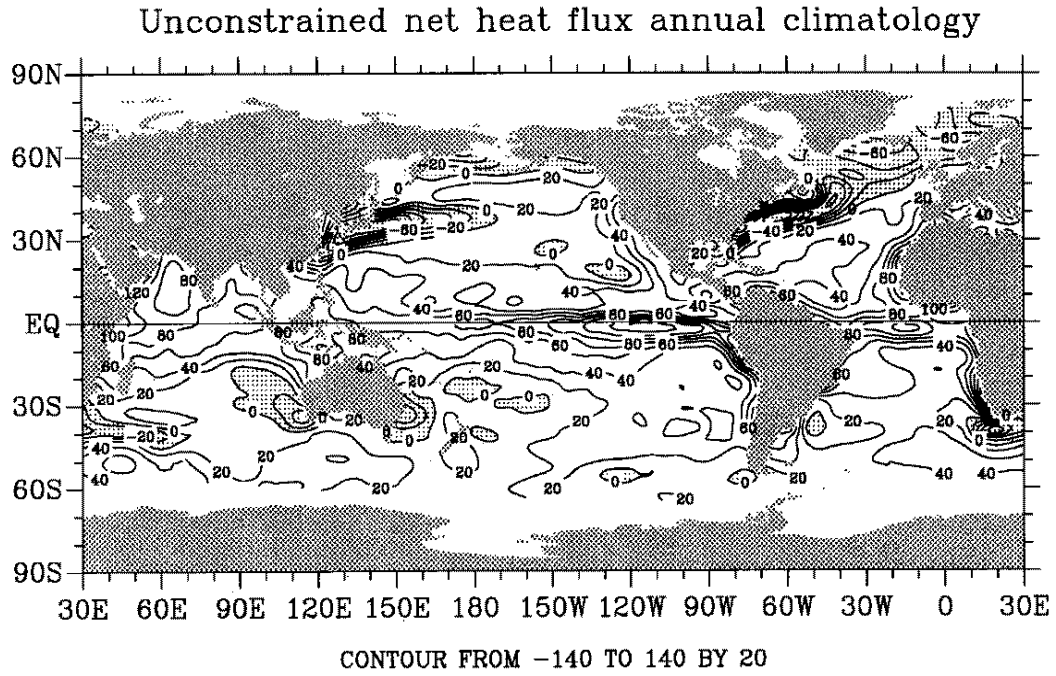

Figure 6: Revised, constrained annual mean net heat flux over the global ocean (W/m^2). Heat flux is computed using the revised beaufort scale with anemometer height reduction to 10 m and constrained so that the global meridional heat transport at the southern boundary is zero.

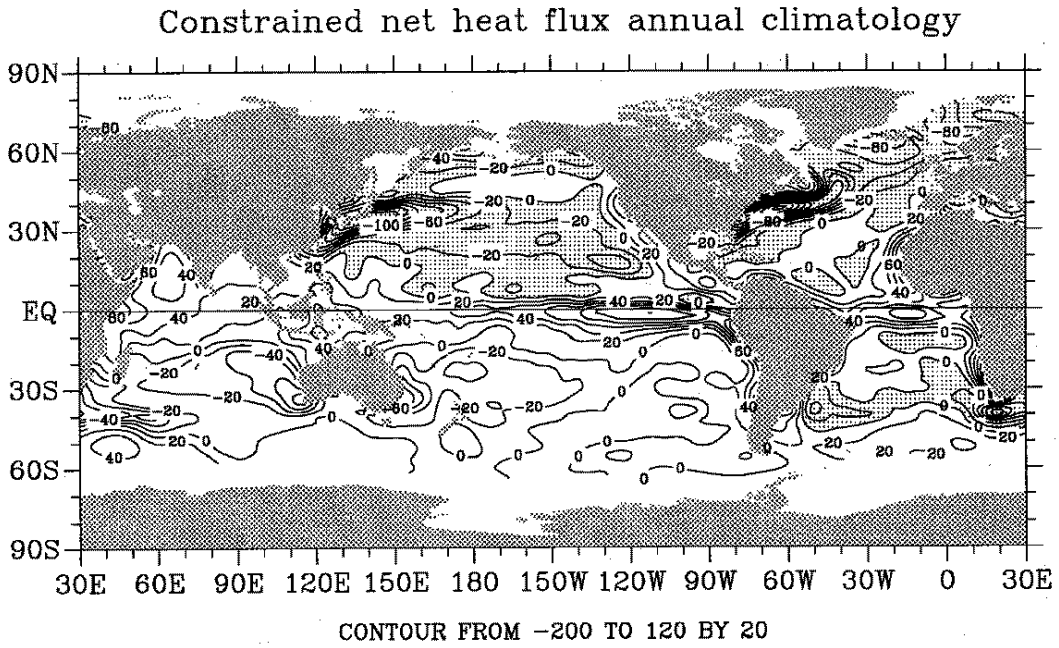

Figure 7: Meridional heat transport(1 PW=10^{15}W) calculated from constrained net heat flux. Heat flux is computed using the revised Beaufort scale with anemometer height reduction of 10 m and constrained so that the global meridional heat transport at the southern boundary is zero. Three oceanographic measurements for Atlantic heat transport are shown with error bars: (R) Rago and Rossby [1987], (H) Hall and Bryden [1982], (W) Wunsch [1984].

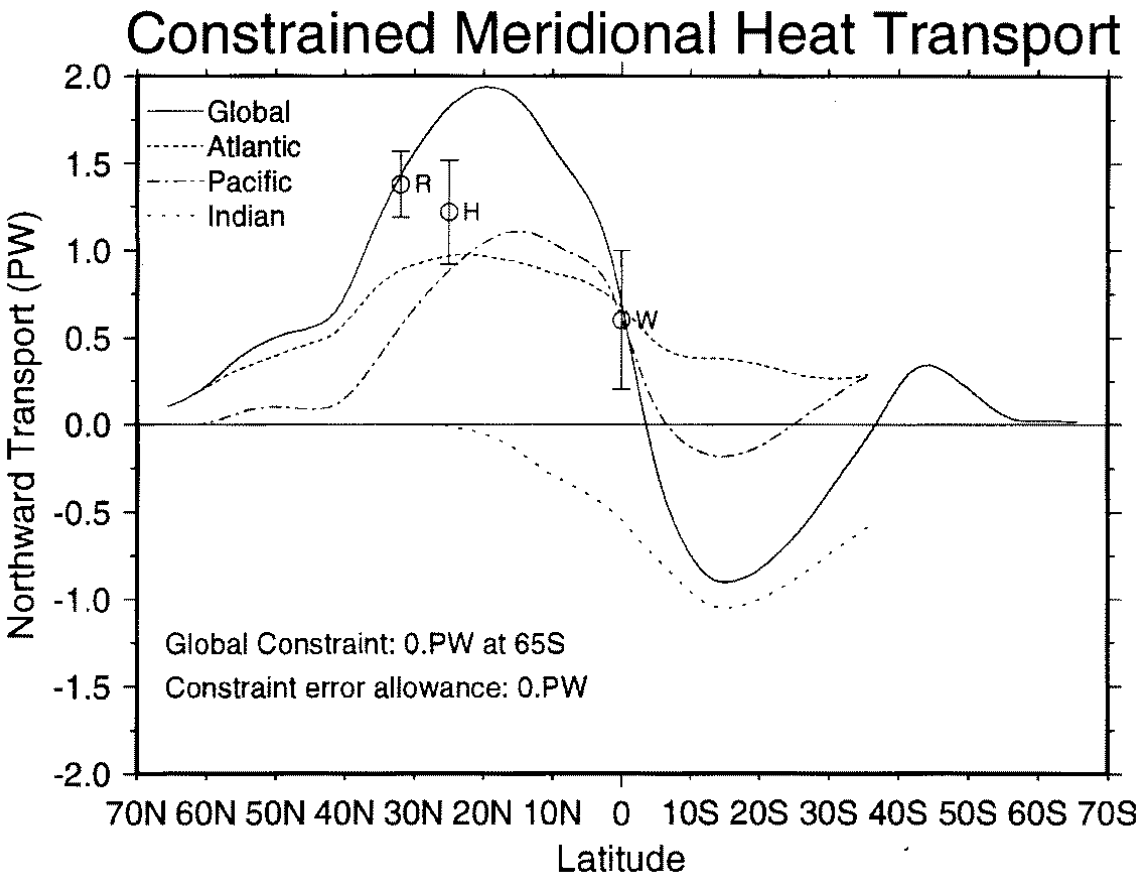

Figure 8: Zonal averages of latent heat flux (W/m^2) over the globe for boreal winter (DJF). Our revised, constrained latent heat flux [solid line] is compared to the latent heat fluxes of Oberhuber et al., (1988) [long dash], Esbensen and Kushnir (1981) [medium dash], and Busalacchi et al., (1993) [short dash].